

## Al Alloys Development Assisted by Thermodynamic Kinetics Phase Field Simulations and Experiments

Nicolas Masquelier<sup>1</sup>, Suzana Gomes Fries<sup>1,2</sup>, Helena Zapolsky<sup>1</sup>, Williams Lefebvre<sup>1</sup>, Renaud Patte<sup>1</sup> and Philippe Pareige<sup>1</sup>

<sup>1</sup> GPM, Université et INSA de Rouen, UMR CNRS 6634, Avenue de l'Université - B.P. 12  
76801 Saint-Etienne du Rouvray, CEDEX, France

<sup>2</sup> ICAMS, STKS, Ruhr-University - Bochum, Stiepelers str 129, D-44801 Bochum, Germany

The coarsening kinetics of  $L1_2$  ( $\gamma'$ ) precipitates in ternary Al-Ti-Zr alloys is studied by using the three-dimensional phase-field simulations. Our focus is on the influence of misfit in the system and the difference of diffusion coefficients for different sort of atoms on the transformation path kinetics from disordered f.c.c. matrix to two phase equilibrium state with  $\gamma'$  precipitates and f.c.c. disordered matrix. The simulation results demonstrate that the  $Al_3Zr$  particles precipitate firstly following by a precipitation of Ti atoms. In this case, Ti atoms diffuse inside of precipitates and form homogeneous  $L1_2$  particles. The coarsening kinetics in Al-Zr-Ti alloys is discussed in comparison with kinetics in Al-Zr-Sc system. Our simulations results are in good agreement with our experimental TEM images and 3D atom probe analyses.

**Keywords:** Phase field, Thermocalc, precipitation kinetics

### 1. Introduction

The Al-Zr-Ti and Al-Sc-Zr systems exhibit particular promise for developing thermally-stable precipitation-strengthened Al alloys. In these systems, upon aging, decomposition of supersaturated solid solutions occurs by the nucleation of  $Al_3Zr_{1-x}M_x$  ( $M=Sc$  or  $Ti$ ) precipitates with a metastable cubic  $L1_2$  structure [1-9] (structurally and chemically analogous to the  $Ni_3Al$  ( $\gamma'$ ) phase in Ni-based superalloys).

Addition of Zr together with Sc to Al matrix improves the effectiveness of Sc as an inhibitor of recrystallization and increases the stability of the alloy during prolonged annealing at high temperatures [10]. This interesting behavior is believed to link to the presence of several kinds of very fine particles [5-9]. The presence of Zr in ternary Al-based alloys reduces the susceptibility of the  $Al_3Sc$  precipitates to coarsening. Recent experimental studies [11] show that the Zr atoms dissolve in the  $Al_3Sc$  phase by replacing of Sc atoms and decrease the lattice parameter of the ordered  $Al_3Sc_{1-x}Zr_x$  phase. By changing the Sc/Zr ratio, it is therefore possible to reduce the lattice parameter mismatch between the  $L1_2$  precipitates and the Al matrix. Zirconium diffuses three orders of magnitude slower than Sc in Al at 375°C and after aging at this temperature the equilibrium structure of precipitates is heterogeneous. The core of ordered precipitates is Sc rich and Zr segregates on the matrix/precipitates interface. Zirconium shell blocks the diffusion of aluminium atoms and changes the coarsening rate. In spite of attractive properties of Al-Sc-Zr alloys, the high price of scandium limits their applications.

Malek et al. [12] have performed an extensive investigation of Al-Zr-Ti system in high supersaturated alloys. They claimed that a partial substitution of Ti for Zr in  $Al_3$  ( $Zr_{1-x}Ti_x$ ) improved the stability of  $L1_2$  and also delays the onset of overaging and the  $L1_2 \rightarrow DO_{23}$  transformation. However, Knipling et al [1-4] didn't find that Al-Zr-Ti alloys improvement of coarsening resistance of  $Al_3Zr$  ( $L1_2$ ) precipitates.

In our study we give some insight on the kinetic of precipitation in ternary Al-Zr-Ti alloys. Using Thermo-Calc<sup>®</sup> [13] calculations we discuss about the domain of stability of  $L1_2$  ordered phase in

these ternary alloys and then using phase field modeling we reproduce the coarsening kinetics. Our simulation results are compared with experimental TEM images and 3D atom probe analyses.

## 2. Thermodynamic description of Al-Zr-Ti alloys.

Thermo-Calc calculations of binary Al-Zr, Al-Ti and Al-Zr-Ti alloys were performed using the software Thermo-Calc with the TTAL6 data-base [14]. The metastable and stable phase diagrams at 475°C of Al-Zr-Ti system are shown in Fig.1. The compositions of studied alloys are indicated by the red crosses. According to metastable phase diagram there is a fcc (A1) + L<sub>12</sub> two-phase field where the L<sub>12</sub> phase is a fcc-based ordered structure. The L<sub>12</sub> order is formed upon cooling as a result of the primary fcc → L<sub>12</sub> ordering followed by the secondary L<sub>12</sub> → DO<sub>22</sub>+DO<sub>23</sub> ordering. In fact, the L<sub>12</sub> phase is thermodynamically less stable than the DO<sub>22</sub> or DO<sub>23</sub> phases at 475°C. However, the L<sub>12</sub> → DO<sub>22</sub> equilibration in Al-Zr-Ti system is so sluggish that in the most of the cases the decomposition and ordering develops in accordance with is the metastable phase diagram. The solubility limits for the L<sub>12</sub>, DO<sub>22</sub>, DO<sub>23</sub> and α(A1) phases are given in Table1. It can be seen from this table that the solubility limit of Zr and Ti in the stable phases is smaller than in the metastable L<sub>12</sub> phase. It means that secondary ordering kinetics will also increase the volume fraction of ordered precipitates.

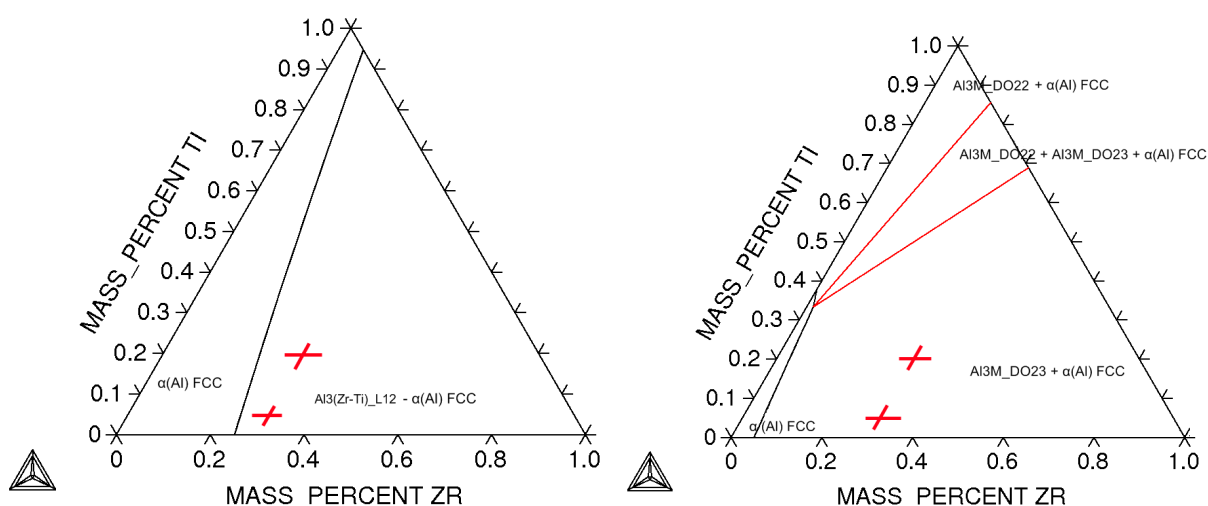


Fig. 1. Metastable and stable phase diagrams at 475°C of the Al rich corner of the Al-Zr-Ti system calculated by THERMO-CALC.

Table 1 Solubility limits of Zr and Ti atoms in α(Al) matrix in binaries Al-Zr and Al-Ti alloys from metastable and stable phase diagrams.

Trialuminide	Solubility limit in α(Al) at 475°C (stable phase)	Solubility limit in α(Al) at 475°C (metastable phase)
Al <sub>3</sub> Zr	0.04%wt Zr (DO <sub>23</sub> phase)	0.24%wt Zr (L <sub>12</sub> phase)
Al <sub>3</sub> Ti	0.4%wt Ti (DO <sub>22</sub> phase)	1.22%wt Ti (L <sub>12</sub> phase)

## 3. Phase field modeling

Phase field model has been extensively used for microstructure simulation studies because of its ability to reproduce complicated microstructures without any a priori assumptions [16]. Two phase microstructure (fcc + ordered L<sub>12</sub> phase) can be described by three long-range order parameters (LRO)  $\eta_1$ ,  $\eta_2$ ,  $\eta_3$ , and a concentration field  $c(r,t)$ . In this method, the microstructural evolution can be obtained by solving the time dependent Ginzburg-Landau equation for the three LRO parameters:

$$\frac{\partial \eta_i(\mathbf{r}, t)}{\partial t} = -L \frac{\partial F}{\partial \eta_i(\mathbf{r}, t)} + \zeta_i \quad i=1, 2, 3 \quad (1)$$

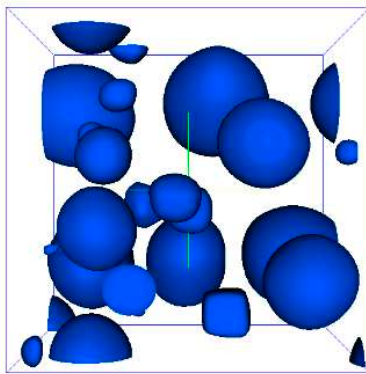
And the non-linear Cahn-Hillard diffusion equation for the concentration field:

$$\frac{\partial c(\mathbf{r}, t)}{\partial t} = \nabla M(\mathbf{r}, t) \nabla \left( \frac{\partial F}{\partial c(\mathbf{r}, t)} \right) + \xi \quad (2)$$

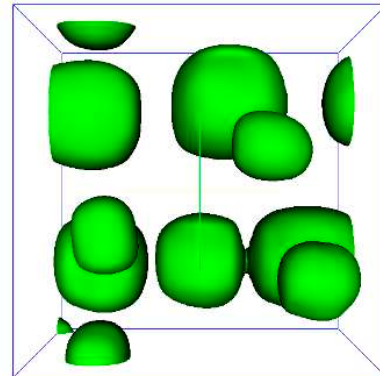
Here  $L$  and  $M$  are kinetic coefficients,  $\zeta_i$  and  $\xi$  are the Langevin's noise terms describing the compositional and structural thermal fluctuations, respectively and  $F$  is a total free energy. For the coherent precipitation under consideration, the total free energy is consist of two terms: elastic strain energy ( $E_{\text{elast}}$ ) and the chemical free energy ( $F_{\text{chem}}$ ), namely  $F = E_{\text{elast}} + F_{\text{chem}}$ . The explicit form for these two terms in the case of ternary alloys has been done in [9]. Our simulations were performed by numerically solving the five nonlinear equations (Eqs (1) and (2)), one for each variable, using the semi-implicit Fourier-Spectral method [15]. The two and three-dimensional simulations were performed with  $128 \times 128 \times 128$  simulation box, respectively.  $\Delta x = \Delta y = \Delta z = 1.0$  (or the grid spacing) were chosen such way that the interface contains enough grid points to remove the artifacts from the underlying discretizing lattice. A uniform time step  $\Delta t$  is chosen equal 0.1 to ensure a stable solution. Periodic boundaries conditions are applied. The lattice misfit between disordered fcc matrix and  $\text{Al}_3\text{Zr}$  and  $\text{Al}_3\text{Ti}$  precipitates was extracted from experimental data [1]. Then, using the solubility limits obtained from our thermodynamic calculations, the coefficient of crystal lattice parameter

extension  $\epsilon_0 = \frac{a_{L12} - a_{A1}}{a_{A1}(c_{A1} - c_{L12})}$  is equal  $\epsilon_{0\text{Zr}} = 0.020$  for  $\text{Al}_3\text{Zr}$  and  $\epsilon_{0\text{Ti}} = 0.18$  for  $\text{Al}_3\text{Ti}$  particles. The

diffusion coefficient ratio of zirconium and titanium atoms in the  $\alpha$  (A1) matrix at  $475^\circ\text{C}$  was calculated using thermodynamic data [1] and equal  $D_{\text{Ti}}/D_{\text{Zr}} = 0.085$ . We studied the transformation path from fcc to fcc+ $L1_2$  two phase state in Al - 4.54at% Zr - 4.44 at% Ti at  $475^\circ\text{C}$ .



a) Isoconcentration of Ti



b) Isoconcentration of Zr

Fig. 2 Simulated microstructure in Al - 4.54 at% Zr - 4.44 at% Ti alloy at  $475^\circ\text{C}$  at reduced time  $t^* = 100000$ .

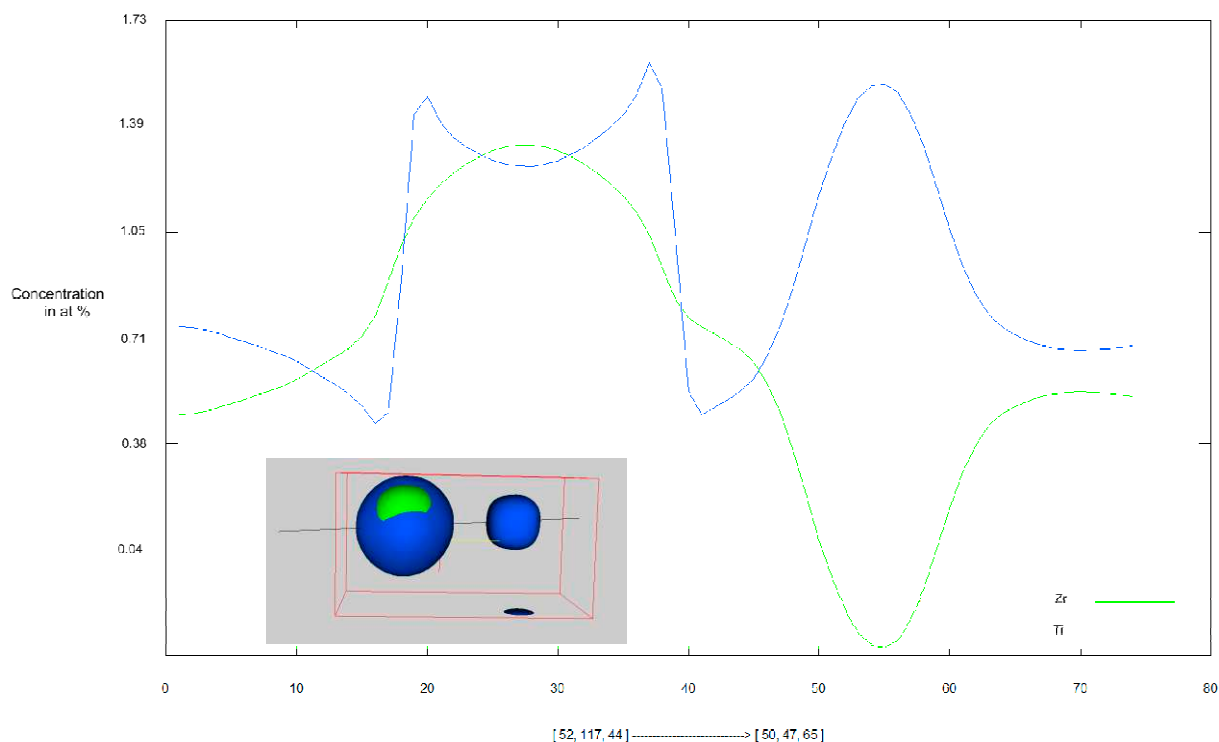


Fig. 3 Concentration profile across of two  $L1_2$  precipitates

The Fig.2 show the isoconcentration of Zr and Ti in Al - 4.54 at% - Zr 4.44 at%Ti alloys at reduced time  $t^*=100000$ . The concentration profile across the  $L1_2$  ordered precipitates is shown in Fig.3. There are two major differences of microstructure in Al-Zr-Ti and Al-Zr-Sc alloys. First, the ordered precipitates in Al-Zr-Ti keep a spherical form at different stages of coarsening. However, in Al-Sc-Zr systems the  $L1_2$  precipitates become cuboidal at very early stages of coarsening. Secondly, in Al-Zr-Ti alloy the Zr and Ti atoms are homogeneous distributed inside of precipitate while in Al-Sc-Zr system ordered particles have an heterogeneous structure where Zr atoms segregate at the interface  $Al_3Sc/\alpha(Al)$  matrix. These differences can be understand from the small value of misfit in Al-Zr-Ti systems with respect to that in Al-Sc-Zr alloys and prove a big influence of elastic energy on stability of heterogeneous structure of precipitates. In Al-Zr-Ti system the Ti atoms diffuse 20 times slowly at  $475^\circ C$  than Zr, this why at the beginning we observe the formation of  $Al_3Zr$  precipitates. This stage is following by the precipitation of Ti atoms. The misfits of both types of ordered particles ( $Al_3Zr$  and  $Al_3Ti$ ) are approximately the same and Ti diffuses inside of precipitates and partially replaces Zr atoms in  $L1_2$  structure. In Al-Sc-Zr system the misfit of  $Al_3Zr$  particles is 1.3 times smaller than that for  $Al_3Sc$  particles and segregation of Zr atoms at the  $\gamma'/\gamma$  interface decreases the elastic energy of system.

Comparing the Fig.2a and 2b we can conclude that at the given coarsening stage there are two types of precipitates. Small particles correspond to the  $Al_3Ti$  precipitates and the big ones have approximately  $Al_3(Zr_{0.5}Ti_{0.5})$  concentration. The concentration profiles in Fig.3 confirm this conclusion.

#### 4. Experimental data

TEM investigations were made to describe the microstructure and precipitates shape in the commercial Al - Zr  $0.4wt\%$  - Ti  $0.03wt\%$  alloy with some small additions. The elaboration of this commercial sample is confidential and can't be described in the paper. These experimental results have been compared with simulation. Using phase field method we can't simulate the low volume fraction of precipitate. In this case the driving force is quite small and the system stays in the disordered state.

Samples were prepared with by mechanical polishing to have a thickness between 80 and 100 $\mu\text{m}$ . Electropolishing using Tenupol were used to prepare a thin. TEM investigations were performed with a JEOL 2000 FX.

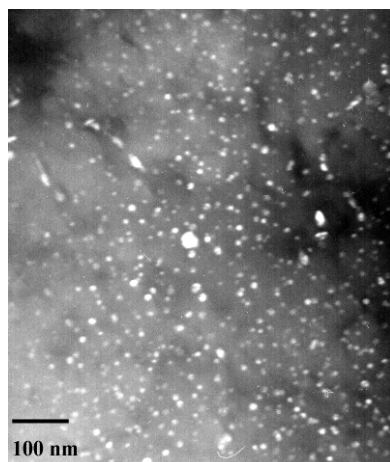


Fig. 4 Dark field image in  $[100]_{\alpha\text{-Al}}$  zone axis selecting reflexion (110) showing  $\text{Al}_3(\text{Ti-Zr})\text{L}_{12}$  precipitate distribution in  $\text{Al} - \text{Zr}_{0.4}\text{Ti}_{0.03}$

Fig.4 shows the dark field image in  $[100]_{\alpha\text{-Al}}$  zone axis selecting reflexion (110). A fine homogeneous distribution of spherical precipitates with  $\text{L}_{12}$  structure is observed. The mean radius was found to be approximately  $\langle r \rangle = 3.7 \pm 1.4$  nm. In combination with TEM, Atom probe tomography (APT) analysis was made to compare our simulated concentration profiles across the precipitates.

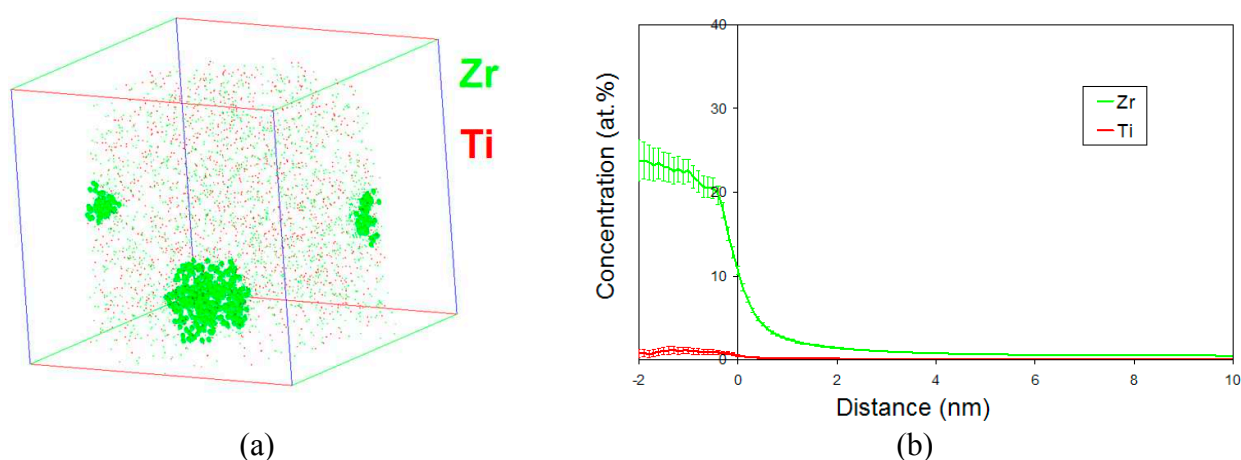


Fig. 5. (a) APT reconstruction showing  $\text{Al}_3(\text{Zr-Ti})$  precipitates (box size:  $40 \times 40 \times 37 \text{ nm}$ ) (b) Erosion profile in a box of  $15 \times 15 \times 20 \text{ nm}$  across the interface of the larger dispersoid observed on the left.

Fig 5 shows 3D reconstruction and erosion profile obtained by APT analysis in an  $\text{Al} - \text{Zr} 0.4\text{wt}\% - \text{Ti} 0.04\text{wt}\%$  alloy. Thanks to the erosion profile across  $\text{Al}_3(\text{Zr-Ti})$  dispersoid, we can see that the distribution of Zr and Ti atoms is homogeneous in  $\text{Al}_3(\text{Zr-Ti})$  precipitates. No core/shell structure was observed. This confirms the observation of Knipling et al [1-4, 12].

## 5. Conclusions

Precipitation in  $\text{Al-Zr-Ti}$  alloys has been investigated. The followed results have been obtained and discussed:

- The microstructure contains the spherical  $\text{L}_{12}$  precipitates homogeneously distributed in the disordered fcc matrix.

- The difference in diffusion coefficients of Ti and Zr atoms in Al matrix is responsible to the existence of two types of precipitates at the later stages of coarsening. The small particles have the composition  $\text{Al}_3\text{Ti}$  and biggest ones have  $\text{Al}_3(\text{Zr-Ti})$
- The distribution of Ti and Zr atoms inside of precipitates is homogeneous.

Our simulation results and our experimental data show a big difference between Al – Zr – Ti [1-4, 12] and Al – Zr – Sc [5-11] in the kinetics of precipitation and in morphology of ordered particles.

## References

- [1] Keith E. Knippling, David C. Dunand, and David N. Seidman. Criteria for developing castable, creep-resistant aluminum-based alloys a review. *Zeitschrift für Metallkunde*, 97(3):246–265, 2006.
- [2] K.E. Knippling, D.C. Dunand, and D.N. Seidman. Atom probe tomographic studies of precipitation in al-0.1zr-0.1ti (at.%) alloys. *Microscopy and Microanalysis*, 13(06):503–516, 2007.
- [3] Keith E. Knippling. Development of a nanoscale precipitation-strengthened creep-resistant aluminum alloy containing trialuminide precipitates. PhD thesis Northwestern university. 2006.
- [4] Keith E. Knippling, David C. Dunand, and David N. Seidman. Precipitation evolution in alzr and al zr ti alloys during isothermal aging at 375425 °c. *Acta Materialia*, 56(1):114–127, 2008.
- [5] B. Forbord, H. Hallem, J. Røyset, and K. Marthinsen. Thermal stability of  $\text{al}_3(\text{sc}_x\text{zr}_{1-x})$ -dispersoids in extruded aluminium alloys. *Materials Science and Engineering: A*, 475(1-2):241 – 248, 2008. International Symposium on Inorganic Interfacial Engineering 2006.
- [6] B. Forbord, W. Lefebvre, F. Danoix, H. Hallem, and K. Marthinsen. Three dimensional atom probe investigation on the formation of  $\text{al}_3(\text{sc},\text{zr})$ -dispersoids in aluminium alloys. *Scripta Materialia*, 51(4):333 – 337, 2004.
- [7] Christian B. Fuller. Temporal evolution of the microstructures of al(sc,zr) alloys and their influences on mechanical properties. PhD thesis Northwestern university. 2003.
- [8] Christian B. Fuller, Joanne L. Murray, and David N. Seidman. Temporal evolution of the nanostructure of al(sc,zr) alloys: Part i chemical compositions of  $\text{al}_3(\text{sc}_x\text{zr})$  precipitates. *Acta Materialia*, 53(20):5401–5413, 2005.
- [9] Julien Boisse. *Modélisation par champ de phase de la cinétique de précipitation dans les alliages Ni-Al, Al-Sc, Al-Zr-Sc*. PhD thesis, Université de rouen, 2008.
- [10] V. V. Zakharov. Effect of scandium on the structure and properties of aluminum alloys. *Metal Science and Heat Treatment*, 45(7):246–253, July 2003.
- [11] Emmanuel Clouet, Ludovic Lae, Thierry Epicier, Williams Lefebvre, Maylise Nastar, and Alexis Deschamps. Complex precipitation pathways in multicomponent alloys. *Nat Mater*, 5(6):482–488, June 2006.
- [12] P. MÅlek, M. Janeoek, B. Smola, P. BartuÅ ka, and J. PleÅ til. Structure and properties of rapidly solidified al-zr-ti alloys. *Journal of Materials Science*, 35(10):2625–2633, may 2000.
- [13] S. G. Fries H. L. Lukas and B. Sundman. *Computational Thermodynamics The Calphad Method*. Cambridge university Press, 2007.
- [14] *Thermotech Database for aluminium alloys 6*, . <http://www.thermocalc.com/TCDATA.htm>
- [15] L.Q. Chen and J. Shen. *Applications of semi-implicit Fourier-spectral method to phase field equations*. Computer Physics Communications. 108. 147-158. 1998.
- [16] L.Q. Chen *Phase-Field Models for microstructural evolution* Annual Review of Materials Research, 2002. 32:p. 113-140
- [17] Thermo-Calc<sup>®</sup>. <http://www.thermocalc.com/Software.htm>